THE TREATMENT OF NONEQUILIBRIUM IN THE TRANSPORT OF HEAT AND MASS IN COMBUSTION IN POROUS MEDIA

Amir A. M. Oliveira (amirol@emc.ufsc.br)
Departamento de Engenharia Mecânica
Universidade Federal de Santa Catarina
Campus Universitário, Caixa Postal 476
CEP 88040-900, Florianópolis, SC, Brazil
Massoud Kaviany (kaviany@engin.umich.edu)
Department of Mechanical Engineering and Applied Mechanics
The University of Michigan
Ann Arbor, MI 48109-2125, U.S.A.

Abstract – *Combustion in inert, catalytic and combustible porous media occurs under the influence of a large range of geometric length scales, thermophysical and thermochemical properties, and flow, heat and mass transfer conditions. As a result, a large range of phenomenological length and time scales control the extent of departure from local thermal and chemical nonequilibrium. Here we summarize the processes leading to these thermal and chemical nonequilibrium, their role in the combustion in porous media, their innovative uses and effects on applications, the current modeling of these processes and the modeling techniques that may allow for further improvements and developments.*

Keywords: porous media, combustion, nonequilibrium, volume averaging, unit cell

1. INTRODUCTION

Porous media may present a large range of pore sizes, porosities, pore connectivities, and specific interfacial areas between phases. The solid phase may range from organic to ceramic and metallic and the fluid phases may have properties ranging from low pressure gases to liquid macromolecules. This combination of a variety of length scales and physical properties allows for large thermal, chemical, and mechanical nonequilibria among and within phases. We can define nonequilibria with the help of Figure 1, that presents a rendering of a multi-length scales porous medium. These nonequilibria are in contrast to the local thermodynamic equilibrium, which is usually assumed to exist at phase interfaces. Local thermal nonequilibrium at a given length scale, say the length scale characterized by the dimension D in Fig. 1, by definition, occurs when the difference among the local temperature of the phases is comparable in magnitude to the temperature difference across the length scale immediately larger, e.g., the macroscopic temperature difference across the medium length-scale L. This results in local heat transfer among phases which

can be sustained through the intraphasic heat transfer or heat generation/consumption. Local chemical nonequilibrium occurs when the difference among the species chemical potential of the phases is comparable in magnitude to the differences across the immediately larger length scale. This results in mass transfer across the interfaces which can be sustained through the intraphase mass transport and chemical reaction. The transport and kinetic resistances may delay or prevent the system of reaching equilibrium within the residence times characteristic of the process. Mechanical nonequilibrium occurs when there are variations in fluid phase pressures comparable in magnitude to the differences across the length scale immediately larger, or as a result of a non zero force balance at solid surfaces. This results in fluid flow and movement of the solid matrix.
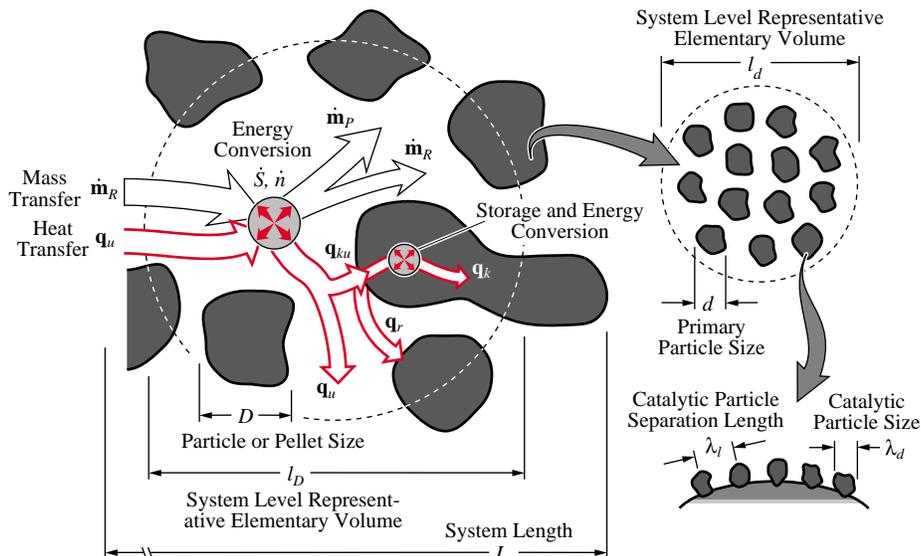

Figure 1: Rendering of a porous media formed by a continuous gas phase and a dispersed solid phase showing the different geometric length scales and the heat and mass transfer processes that may take place in the gas and solid phases.

Nonequilibria are a consequence of the intrinsic characteristics of the medium, e.g., nonuniform distribution of reactants, noncontinuous solid phase, large mismatch between the thermal properties of the fluid and solid phases, or a consequence of the process to which it is subjected, e.g., fast transients, highly endothermic or exothermic reactions and large variations in the inlet and outlet conditions. The possibility of nonequilibrium allows for redistribution of heat and reactants over large sections of the medium, energy storage and recirculation, enhanced reaction rates and the formation and freezing of metastable solid phases. This results in many advantages in using a porous media in combustion systems, but also poses special challenges for the modeling of these processes. The volume-average models tend to filter out the detailed information at the pore-level. In most cases, to detect important nonequilibria, one must use detailed local simulations, either using continuum models or molecular simulation. Also, in face of the difficulties in obtaining measurements at a pore level, the detailed local simulations have filled in the gaps in the understanding of the physics at the pore-level and its interactions with the macroscopic average variables.

Nowadays, many solutions for pore-level (or particle-level) and system-level problems through the use of average continuum models (e.g., volume-average models) and detailed local simulations have become available. They point out to the need of combining both modeling strategies in approaching a problem towards the development of new and inno-

vative engineering solutions.

In the following, we review the characteristics of porous media leading to thermal and chemical nonequilibrium, the modeling with volume-averaged continuum equations and the need for detailed local simulations. Some examples in which thermal and chemical nonequilibrium is desired or may prevent the obtention of an end result are presented.
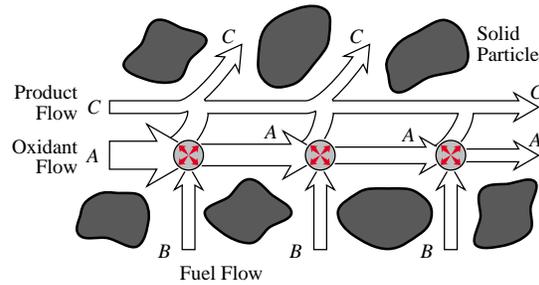
2. DESCRIPTION AND MODELING

Physically, a porous medium is formed by a solid phase and one or more fluid phases. The solid may have a periodic or random structure and each phase may be continuous or dispersed. Figure 1 presents a rendering of a porous medium formed by a continuous gas phase and a dispersed solid phase. The characteristic sizes of the geometric heterogeneities may span multiple length scales. These length scales can either differ by orders of magnitude (i.e., they are separated) or they may vary almost continuously in order of magnitude (i.e., they are continuous). For particulate media, the geometric heterogeneities are the result of large differences in particle sizes and nonuniform distribution and agglomeration of particles with different sizes. For continuous media (e.g., wire meshes, foams, etc.), the heterogeneities are the result of size, aspect ratio and spatial distribution of the solid wires. Chemically, the solid phase may be either inert or it may participate directly in the reactions as a catalytic surface or a source of fuel. Figure 1 also represents the different heat (convection $\mathbf{q}_u$, interphase $\mathbf{q}_{ku}$, conduction $\mathbf{q}_k$ and radiation $\mathbf{q}_r$) and mass (generically shown as reactants $\dot{\mathbf{m}}_R$ and products $\dot{\mathbf{m}}_P$) flux vectors, and the energy and mass conversion and storage (energy conversion $\dot{S}$, mass conversion $\dot{n}$) that are used to describe the transport and reaction during combustion in porous media. For inert media, the geometric characteristics result from the manufacturing, and for combustible media, they appear as a consequence of the combustion process (e.g., solid combustion, phase change, phase crystallization, growth and coalescence, etc.). Finally, the phases may be permanently continuous or may change with the reaction and a percolation threshold may be reached in which the transport of heat or mass along a phase is interrupted.

These physical and chemical processes have phenomenological length and time scales, such as flame thickness, penetration depth, residence time, etc. The phenomenological length scales can be of the same order of magnitude or much different from the geometric length scales. The interaction among the different phenomenological length and time scales and the geometric scales, results in different transport and reaction regimes and leads to thermal and chemical nonequilibria. Figure 2 shows different examples of pore-level and system-level chemical nonequilibrium. They are classified accordingly to the distribution and to the physical process controlling the mixing of reactants. Fig. 2(a) is characteristic of the combustion of premixed gas mixtures inside a porous medium, as in the porous radiant burners [1-8,23,48,49], catalytic converters [9,10] and combustors [11-16], and energy regeneration devices [17-22]. Note that the solid phase may be either chemically inert or catalytic and both homogeneous and heterogeneous reactions may take place. The flow of reactants and products may be either pressure or diffusion driven. Only the last scale with a nonporous solid phase is represented. In Fig. 2(b) a porous burner for which the fuel supply is noncontinuous is depicted. This is useful in controlling the amount of heat generated per unit volume (or area) of the porous burner either to satisfy the demand for heat (the heat is radiated out from the burner surface) [23] or to control the maximum temperature in the burner [24]. The flow of reactants is pressure driven and good mixing is usually assumed. Figure 2(c) presents the case in which the fuel is provided from the pyrolysis of the solid, as in solid combustion or smoldering [28-31] and
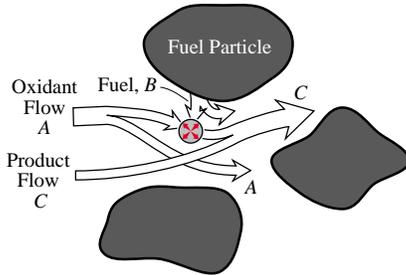
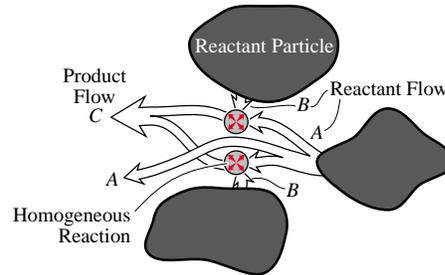**(a) Homogeneous and Heterogeneous Reaction with Premixed Oxidant and Fuel Supply**

Heterogeneous Reaction
Solid Particle
Catalytic Surface
Reactants Flow $A+B$
C
Product Flow C
$A+B$
Homogeneous Reaction
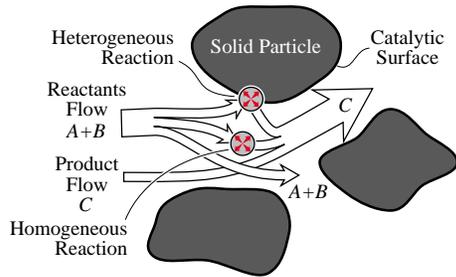
(b) Homogeneous Reaction with Continuous Oxidant and Distributed Fuel Supply

C C Solid Particle
Product Flow C C
Oxidant Flow A A A A
B B B
Fuel Flow

(c) Homogeneous Reaction with Transport Controlled Fuel Supply

Fuel Particle
Oxidant Flow A Fuel, B
C
Product Flow C
A

(d) Homogeneous Reaction with Transport Controlled Oxidant and Fuel Supply

Reactant Particle
Product Flow C
B Reactant Flow
A
A
B
Homogeneous Reaction

(e) Homogeneous and Heterogeneous Reaction with Transport Controlled Oxidant Supply or Product Removal

B
Homogeneous or Heterogeneous Reaction
Product Flow C
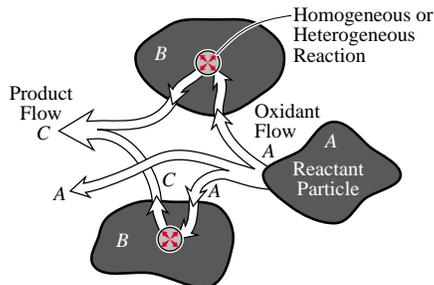Oxidant Flow A
A
Reactant Particle
A
C A
B

Figure 2: Distribution and transport of reactants and chemical reaction in chemical nonequilibrium processes.

particulate trap regeneration [32,33], or from evaporation of liquid in the form of droplets [25,26]. In this case, the rate of pyrolysis or evaporation may control the reaction. The reaction could also occur inside the solid phase (not depicted) and controlled by the transport of oxidizer or products. Figure 2(d) shows an example in which both the reactants come from the solid particles (of different materials), with the reaction occurring in the gas phase. This may be the case of some solid and condensed-phase combustion synthesis [36, 37]. The reactants mixing may be controlled by the rates of generation or by mass transfer. The product in the liquid or gas phase can then nucleate and crystallize as a solid product. Finally, Fig. 2(e) shows the reaction occurring inside one of the reactant particles, as in gasless combustion synthesis [34-40]. The reactants mixing is controlled by the transport in the pore space (by diffusion or capillarity) and within the reactant B particle (by diffusion). The product may be in the solid phase, growing around the reactant B particle, or in the liquid phase, later nucleating and growing as

a solid phase. These mixing effects depicted in Fig. 2(a) to (e) can be manipulated to some extent. For example, the control of the distribution of fuel in a porous burner leads to distributed heating [23]. In another example, the maximization of reactant mixing in combustion synthesis by controlling the particle size and particle size distribution leads to higher conversion rates [38, 39]. To better control the geometry of the medium and the processes occurring there, a fundamental understanding of the interaction among the various processes and scales is needed.

2.1 Modeling

When the scales are sufficiently separated, the use of continuum (or volume-averaged, or homogeneous) models is common. Otherwise, when there is an almost continuous variation of length scales, detailed local simulation is needed.

The volume-averaged models are obtained from the averaging of the point-wise conservation equations, starting with two phases β and σ in contact and for which the continuum hypothesis and the thermodynamic equilibrium at phase interfaces hold. Here, we will not consider turbulent fields and the need for time-averaging. The conservation of mass of the chemical species i is written for a multicomponent mixture [55]. In most problems, temperature (Soret effect), pressure and body force driven diffusion are neglected. The mass jump condition at the phase interface is written usually neglecting absorption and surface transport at the interface. In the energy equation, usually viscous dissipation, pressure work, and body forces are neglected. The energy equation is written, in general, in an enthalpy form. However, for a small number of components and chemical reactions, it can be conveniently written in a temperature form. Usually, the concentration gradient driven heat flux (Dufour effect) is neglected. In the energy jump condition energy accumulation and transport at the interface are generally neglected. These equations are completed with the conservation of linear momentum equations and the boundary conditions at inlet and outlet of each phase in the macroscopic domain of interest.

Rigorous derivations of volume-averaged conservation equations are available when the phase interfaces are stationary, for binary mixtures and in the absence of cross effects [41-47] . The intrinsic phase-average of a scalar or vector quantity ϕ_β is defined as the volume average of that quantity for phase β over the volume V_β occupied by phase β inside an elementary representative volume, $V = V_\beta + V_\sigma$, i.e.,

$$\langle \phi_\beta \rangle^\beta \equiv \frac{1}{V_\beta} \int_{V_\beta} \phi_\beta dV = \frac{1}{\varepsilon_\beta} \left(\frac{1}{V} \int_{V_\beta} \phi_\beta dV \right) \equiv \frac{1}{\varepsilon_\beta} \langle \phi_\beta \rangle \tag{1}$$

where $\varepsilon_\beta = V_\beta/V$ is the volume fraction occupied by phase β. The choice of the size of the elementary representative volume V is such that it is large compared to the pore- (or particle-) level geometric and phenomenological length scales but small compared to the system-level geometric and phenomenological length scales. Naming l the characteristic dimension of the representative elementary volume, these conditions can be expressed as

$$d \ll l \ll L, \qquad \delta_{i,l} \ll l \ll \delta_{i,L} \tag{2}$$

where δ_i are the different phenomenological length scales at the l and L geometric scales. For example, for a catalytic reaction inside a porous radiant burner, l should be much larger than the mass boundary layer thickness $\delta_{y,l}$ inside a pore, to be able to capture the bulk rate of conversion of reactants. However, to capture the entrance effects, l should be smaller than the pore entrance length $\delta_{x,l}$ and this is usually not met, because the

entrance length for the chemically reacting flow is of the order of magnitude of the pore diameter ([12, 15]). In another example, in combustion synthesis, large concentration gradients, comparable to the system-level concentration gradients, are developed at a particle-level and a single representative elementary volume cannot also be defined ([38-40]). At any rate, we can attempt to define a representative volume for a given length scale and integrate the equations inside this volume, then filtering out any process occurring at the smaller scales. The volume-averaged equations thus obtained end up containing terms with the average of the product of velocity and temperature $\langle \mathbf{u}_\beta T_\beta \rangle^\beta$ or velocity and mass concentration $\langle \mathbf{u}_\beta \rho_\beta \rangle^\beta$. To develop closure relations, it is common to express the deviation of the local field in respect to the average field for any scalar or vector, generically denoted as ϕ'_β, by

$$\phi'_\beta = \phi_\beta - \langle \phi_\beta \rangle^\beta \tag{3}$$

Then, a constitutive relation for the average of deviations become necessary. The most severe assumption used to arrive at these closure equations is the assumption of a linear relation between fluctuations and the gradient of average quantities. For example, for a scalar field, one could specify ([47])

$$\phi'_\beta = \mathbf{b}_{\beta\beta} \cdot \nabla \langle \phi_\beta \rangle^\beta + \mathbf{b}_{\beta\sigma} \cdot \nabla \langle \phi_\sigma \rangle^\sigma + \psi_\beta \left(\langle \phi_\sigma \rangle^\sigma - \langle \phi_\beta \rangle^\beta \right) + \xi_\beta \tag{4}$$

where $\mathbf{b}_{\beta\beta}$, $\mathbf{b}_{\beta\sigma}$, ψ_β and ξ_β are vector and scalar fields to be determined by the solution of one or more closure problems.

Constitutive relations as this one should reflect the variations occurring at the smaller scales. The linear approximation above is strictly valid only for small variations of the field of fluctuations when compared to the variations of the averaged values and for short relaxation times at the local scale. We have seen above that this may not be true, depending on the importance of entrance lengths and boundary layer thicknesses in the process under consideration. To arrive at closure relations for these situations, we would need to use higher order expansions for the field of fluctuations, which would easily become mathematically involved. Another alternative is to attempt a solution for the particle- and pore-level problem and then connect this solution to the volume-averaged equations through the source terms. The solution for the local problem can rely on a simpler set of boundary conditions when there is sufficient separation of length scales. This is the nature of shrinking-core models for reactions in beds of catalytic particles, or small-droplet evaporation models for spray or particle combustion. When there is not sufficient separation, detailed numerical simulation of the entire system-level domain is necessary. This is particularly the case for catalytic reactions in high temperature, short catalytic burners ([12,15,16]).

2.2 Volume-Averaged Treatment

For those problems conveniently characterized by a separation of length scales, two- (and three-) medium treatments are developed to model the nonequilibrium among phases. For example, for the system composed of phases β and σ, two intrinsic volume-averaged equations are needed. The equation for the conservation of a chemical species i in the β phase has been commonly written as

$$\frac{\partial}{\partial t} \langle \rho_i \rangle^\beta + \nabla \cdot \left[\langle \rho_i \rangle^\beta \langle \mathbf{u} \rangle^\beta - \langle \rho \rangle^\beta \left(\mathcal{D}_{i,e}^\beta + \mathcal{D}_m^\beta \right) \nabla \frac{\langle \rho_i \rangle^\beta}{\langle \rho \rangle^\beta} \right] = \langle \dot{n}_{r,i} \rangle^\beta \tag{5}$$

where $\mathcal{D}_{i,e}^{\beta}$ is the effective multicomponent diffusivity of species i in the mixture, $\mathcal{D}_{m}^{\beta}$ is the mass dispersion coefficient and $\langle \dot{n}_{r,i} \rangle^{\beta}$ is the volume-averaged reaction rate. Allowing for both homogeneous in the bulk $\langle \dot{n}_{r,i} \rangle_{\beta}^{\beta}$ and heterogeneous reaction at the $\beta\sigma$ interface $\langle \dot{n}_{r,i} \rangle_{\beta\sigma}^{\beta}$, the intrinsic phase averaged reaction rate for phase β can be modeled as

$$\langle \dot{n}_{r,i} \rangle^{\beta} = \langle \dot{n}_{r,i} \rangle_{\beta}^{\beta} + \langle \dot{n}_{r,i} \rangle_{\beta\sigma}^{\beta} \tag{6}$$

where, by defining $\langle \phi_i \rangle^{\beta\sigma}$ as the area-average of ϕ_i on the $\beta\sigma$ interface and using $S_{\beta\sigma} = A_{\beta\sigma}/V$ for the specific surface area of the $\beta\sigma$ interface,

$$\langle \dot{n}_{r,i} \rangle_{\beta\sigma}^{\beta} = -\langle \dot{m}_i \rangle^{\beta\sigma} \frac{S_{\beta\sigma}}{\varepsilon_{\beta}} \tag{7}$$

The interfacial jump condition can be averaged to give

$$\langle \dot{m}_i \rangle^{\beta\sigma} = (\langle \dot{\mathbf{m}}_i \rangle^{\sigma} \cdot \mathbf{n}_{\beta\sigma})_{\beta\sigma} \tag{8}$$

where $\langle \dot{\mathbf{m}}_i \rangle^{\sigma}$ is the average mass flux vector at the σ phase. The interfacial mass flux of component i at the $\beta\sigma$ interface has been usually modeled as

$$\langle \dot{m}_i \rangle^{\beta\sigma} = \frac{\mathrm{Sh}_{\beta}\mathcal{D}_{i,m}}{D_{\beta}} \left(\langle \rho_i \rangle^{\beta} - \langle \rho_i \rangle^{\beta\sigma} \right) \tag{9}$$

where Sh_{β} is the interfacial average Sherwood number based on the surface characteristic dimension D_{β}, $\mathcal{D}_{i,m}$ is the multicomponent diffusivity of species i in the mixture m, and $\langle \rho_i \rangle^{\beta\sigma}$ is the concentration of i at the $\beta\sigma$ interface, i.e., $\langle \rho_i \rangle^{\beta\sigma} = (\langle \rho_i \rangle^{\sigma})_{\beta\sigma}$. The use of dispersion coefficients and interphase mass-transfer equations like Eq. (9) relies on the kind of linear constitutive relations discussed above. These have been extended to more general situations through the *empirical modeling* of the dispersion and interfacial transfer coefficients. The derivation of the volume-averaged equations shows the correct form and limitations in the use of interfacial flux equations, dispersion fluxes and effective properties.

The local thermal non-equilibrium is also modeled using two- and three-medium treatments. Assuming that it is transparent to thermal radiation, the thermal energy equation for phase β is commonly written as

$$\frac{\partial}{\partial t} \left(\langle \rho c_p \rangle^{\beta} \langle T_{\beta} \rangle^{\beta} \right) + \nabla \cdot \left[\langle \rho c_p \rangle^{\beta} \langle \mathbf{u}_{\beta} \rangle^{\beta} \langle T_{\beta} \rangle^{\beta} - \left(\langle k \rangle^{\beta} + \langle \rho_{\beta} \rangle^{\beta} c_{p,\beta} \mathcal{D}_T^{\beta} \right) \nabla \langle T_{\beta} \rangle^{\beta} \right] = \langle \dot{s}_{\beta} \rangle^{\beta} \tag{10}$$

where $\langle k \rangle^{\beta}$ is the effective thermal conductivity and $\mathcal{D}_T^{\beta}$ is the thermal dispersion coefficient for phase β. One additional difficulty on writing these equations is the treatment of the heat source/sink at the phase interfaces. A simpler treatment, consists in modeling the volumetric energy generation, in the presence of interfacial heat transfer and homogeneous chemical reaction, as

$$\langle \dot{s}_{\beta} \rangle^{\beta} = \frac{S_{\beta\sigma}}{\varepsilon_{\beta}} \frac{\mathrm{Nu}_{\beta}k_{\beta}}{D_{\beta}} \left(\langle T_{\beta} \rangle^{\beta} - \langle T_{\sigma} \rangle^{\sigma} \right) + \sum_{i=1}^{N_c} \langle n_{r,i} \rangle_{\beta}^{\beta} \Delta h_{r,i} \tag{11}$$

where Nu_{β} is the interfacial average Nusselt number based on D_{β}.

Then, for phase σ, assuming it is stationary, we have

$$\frac{\partial}{\partial t} \left(\langle \rho c_p \rangle^{\sigma} \langle T_{\sigma} \rangle^{\sigma} \right) + \nabla \cdot \left[-\langle k \rangle^{\sigma} \nabla \langle T_{\sigma} \rangle^{\sigma} + \langle q_r \rangle^{\sigma} \right] = \langle \dot{s}_{\sigma} \rangle^{\sigma} \tag{12}$$

where the volumetric energy generation, assuming that there is both homogeneous and heterogeneous chemical reaction at the $\beta\sigma$ interface, is

$$\langle \dot{s}_\sigma \rangle^\sigma = -\frac{S_{\beta\sigma}}{\varepsilon_\beta} \frac{\mathrm{Nu}_\beta k_\beta}{D_\beta} \left(\langle T_\beta \rangle^\beta - \langle T_\sigma \rangle^\sigma \right) + \sum_{i=1}^{N_c} \left(\langle n_{r,i} \rangle^\sigma_\sigma + \langle n_{r,i} \rangle^\sigma_{\beta\sigma} \right) \Delta h_{r,i} \tag{13}$$

where,

$$\langle \dot{n}_{r,i} \rangle^\sigma_{\beta\sigma} = -\langle \dot{m}_i \rangle^{\beta\sigma} \frac{S_{\beta\sigma}}{\varepsilon_\sigma} \tag{14}$$

In the model above, it has been assumed that the interface is part of the σ phase. Thus, the heterogeneous reaction $\langle n_{r,i} \rangle^\sigma_{\beta\sigma}$ occurs in the σ phase, causing heating or cooling of the interface, and then there is heat transfer to the β phase by interphase heat transfer.

The modeling of the problems for which the multiple length scales are separated, employs the simultaneous use of the equations above for all the length scales. Examples of systems for which separation of length scales exist are catalytic reactors and converters, combustion of solid fuels (except pulverized), and combustion synthesis. The connection between an equation for a level and the equations for the levels immediately below is done through the source term. For example, phase σ may also be porous, having a fluid phase γ and a solid phase ψ, and being characterized by smaller characteristic length scales. Interfacial mass fluxes then occur across the various areas available for flow (micro channels) and heterogeneous reactions may occur at the exposed solid surfaces. An initial difficulty is the definition of the interface position, especially, where the interface should be located at the pore mouths, where the fluid phase is in fact continuous. Depending on how much the interface penetrates the pores, a larger part of the surface solid area will be in direct contact with the β phase. Also, locally there could exist strong and recirculating convection flows. The transition between a porous and plain medium was discussed elsewhere, in the context of convection and diffusion [47]. Here, we will assume that we can define an interface region as a sharp interface (in a way, similar to the Gibbs model for interfaces). Assuming no interaction among the fluxes leaving the $\beta\gamma$ and the $\beta\psi$ interfaces, for a porous phase σ, the interfacial mass transfer can be written as

$$\langle \dot{m}_i \rangle^{\beta\sigma} = -f_{\beta\gamma} \langle \dot{m}_i \rangle^{\beta\gamma} - (1 - f_{\beta\gamma}) g_\psi \langle \dot{n}_i \rangle^{\beta\psi} \tag{15}$$

where $f_{\beta\gamma} = S_{\beta\gamma}/S_{\beta\sigma}$ and g_ψ is the apparent fraction of the $\beta\psi$ interface covered by catalytic sites.

If phase ψ is also porous (the third level), being formed by a fluid phase δ and a solid ω, the interfacial mass transfer is then written as

$$\langle \dot{m}_i \rangle^{\beta\sigma} = -f_{\beta\gamma} \langle \dot{m}_i \rangle^{\beta\gamma} - (1 - f_{\beta\gamma}) \left[f_{\gamma\delta} \langle \dot{m}_i \rangle^{\beta\delta} + (1 - f_{\gamma\delta}) g_\omega \langle \dot{n}_i \rangle^{\beta\omega} \right] \tag{16}$$

The mass fluxes at the $\beta\gamma$ and $\beta\delta$ interfaces are

$$\langle \dot{\mathbf{m}}_i \rangle^\gamma = \langle \rho_i \rangle^\gamma \langle \mathbf{u} \rangle^\gamma - \langle \rho \rangle^\gamma D^\sigma_{i,e} \nabla \frac{\langle \rho_i \rangle^\gamma}{\langle \rho \rangle^\gamma}, \qquad \langle \dot{\mathbf{m}}_i \rangle^\delta = \langle \rho_i \rangle^\delta \langle \mathbf{u} \rangle^\delta - \langle \rho \rangle^\delta D^\psi_{i,e} \nabla \frac{\langle \rho_i \rangle^\delta}{\langle \rho \rangle^\delta} \tag{17}$$

and the surface reaction rate $\langle \dot{n}_i \rangle^{\beta\omega}$, for N_r reactions j, is

$$\langle \dot{n}_{r,i} \rangle^{\beta\omega} = M_i \sum_{j=1}^{N_r} \nu_{i,j} \dot{n}_{r,j,\omega} \tag{18}$$

where $\dot{n}_{r,j,\omega}$ is the reaction rate for reaction j occurring at the ω surface and $\nu_{i,j}$ is the stoichiometric coefficient of component i in reaction j (with $\nu_{i,j} < 0$ when i is a reactant). Note also that $\langle \dot{n}_{r,i} \rangle^{\beta\omega} \equiv \langle \dot{n}_{r,i} \rangle^{\beta\psi}$.

This cascade of fluxes is interrupted when an interface and both neighboring phases are in thermal and chemical equilibrium. At this last level, equilibrium equations are written for closure. However, the use of a surface average for this last scale may still be necessary. The surface reaction rate assumes the existence of N_r chemical reactions between N_c chemical species. These reactions occur at crystallites which may be nonuniformly distributed on the surface of the solid particles. The parameters g_ω and g_ψ remain as empirical parameters. The catalytic sites on the crystallites may also vary in activity. For example, the activity of noble metal crystallites depends on lattice orientation, presence of neighboring sites, interaction with the substrate, poisoning, etc. These form the last geometric length scales of interest here. Figure 3 shows a summary of these length scales and characteristic dimensions for various systems.
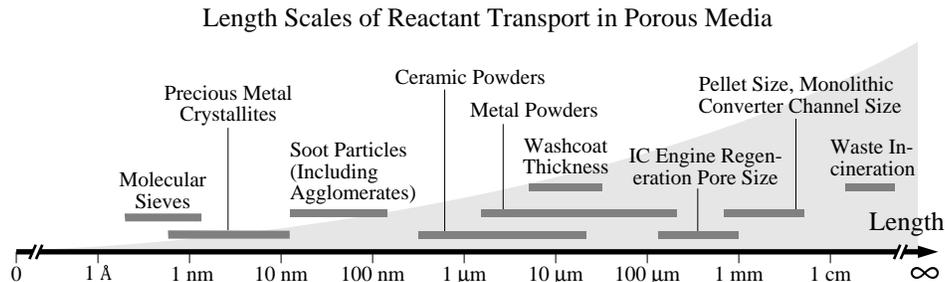

Figure 3: Length scales and characteristic dimensions for various systems.

In the following, an example of systems with important chemical non equilibrium is given and the need for detailed simulation is discussed in that context.

3. CHEMICAL NONEQUILIBRIUM IN CATALYTIC COMBUSTION

Chemical nonequilibrium may be imposed on the system to control combustion and heat transfer, for example, in distributed porous burners, or it may be a result of the inherent characteristics of the system, as in, for example, catalytic reactors, solid pyrolysis and combustion synthesis. Of special concern in the modeling of chemical non-equilibrium, is the accuracy of continuous models in describing transport and reaction in porous media. The questions are whether the effective diffusivity is a function of the reaction rate, if use of an effective diffusivity fails near percolation thresholds and whether it is accurate enough in modeling diffusion of molecules with diameters approaching the pore size. The continuum models agree with network results when the multiscales are taken into account [50]. The use of network models (Zhang and Seaton [52]) has shown that the effective diffusivity calculated in absence of reaction is equal to the one calculated with reaction, as long as there is sufficient penetration of the diffusion front into the modeled network. This is due to the fact that the continuum model fails when the length scale for the penetration is of the same order of magnitude as the pore length. The continuum model also fails near the threshold for percolation caused by pore blockage during poisoning. The correlation length (i.e., the length scale over which the fluid phase is connected) is given by [51]

$$\xi \sim |P - P_c|^{-\upsilon}, \tag{19}$$

where P is the probability of a single pore being blocked, P_c is the critical probability (probability at the percolation threshold) and υ is an exponent which depends on the dimensionality ($\upsilon = 0.88$ for a three-dimensional network). The correlation length tends to infinity when the percolation threshold is reached and, therefore, becomes much larger than the system length L. As the pore size reaches the size of the molecules, a threshold for percolation may also be reached. From the results of Zhang and Seaton, these trends are summarized in Fig. 4(a). The Thiele modulus ϕ_l is defined as

$$\phi_l = \frac{l^2 a_1}{\langle \mathcal{D}_m \rangle} \frac{S_{\beta\sigma}}{\epsilon_\beta}, \tag{20}$$

where a_1 is the reaction rate constant (in m/s) and l is the pore length. For a smooth cylindrical pore with radius r_p, $S_{\beta\sigma}/\epsilon_\beta = 2/r_p$.
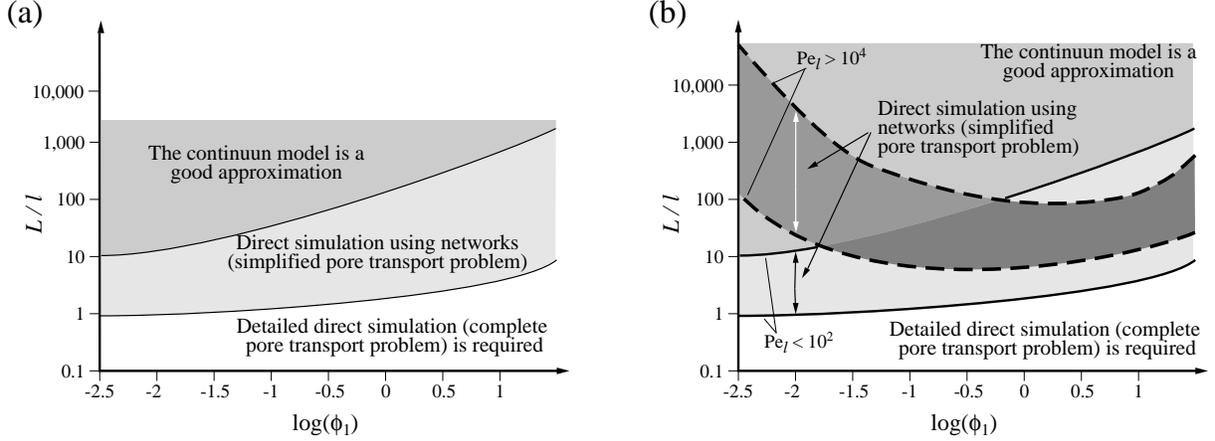

Figure 4: Domains for the modeling of the diffusion and reaction in a porous pellet for (a) uniform reaction rate constants, and (b) nonuniform reaction rate constants. ϕ_l is the pore Thiele modulus and L/l is the ratio of system to pore lengths.

In the model of Zhang and Seaton [52], the reaction rate constant was uniform for the network. In many cases, there may be a nonuniformity in reaction constants due to variations in crystallite distribution and crystallite activity (related to size, shape, surface state, poisoning, etc.). These nonuniformities have their own characteristic length scales which vary from crystallite, to pore, to system size. When the nonuniformity is very pronounced, a percolation threshold may also be reached. It has been shown ([53]) that for uniform reaction constants, the dispersion coefficient (which accounts fo the effect of effective diffusivity and flow in the spreading of a chemical species) is not a function of reaction rate (i.e., it is purely hydrodynamic) and the effective reaction constants are equal to the pore-level ones. However, when the reaction constants are nonuniform, the dispersion coefficient becomes a function of the reaction rate when the characteristic Damköhler number (where u is the pore average velocity and $a = a_2/a_1$ is the chemical equilibrium constant for an adsorption/desorption reaction)

$$\mathrm{Da}_l = \frac{l a^2 a_1}{u} \frac{S_{\beta\sigma}}{\epsilon_\beta}, \tag{21}$$

is small ($\mathrm{Da}_l \to 0$). This condition is reached, for example, when the pore level Peclet number ($\mathrm{Pe}_l = ul/\mathcal{D}_m$) is large or when the reaction rates are small. Alvarado et al. showed that for large Peclet numbers ($\mathrm{Pe}_l > 10^4$), the transport and reaction is dominated

by both convection and reaction. When $Pe_l \rightarrow 0$, diffusion dominates, and the reaction and transport effects are decoupled. Also, when the system size becomes very large ($L \gg l$) the dispersion coefficient approaches a purely hydrodynamic behavior. The Damköhler number is proportional to the ratio of the Thiele modulus and Peclet number, $Da_l \sim \phi_l / Pe_l$. Thus, in the presence of flow, a small Thiele modulus may also require detailed simulation, as summarized in Fig. 4(b). A pore with a fractal surface (large $S_{\beta\sigma}$) would increase the Thiele modulus and a surface effectiveness, which accounts for the accessibility of the surface to the gas molecules, can be defined. Coppens and Froment [54] show that the surface effectiveness of the fractal pore is smaller than the one for a circular pore with the same length. They also conclude that it is usually impossible to construct a smooth cylindrical pore which results in the same flux and end concentrations of a reactant species as the pore with a fractal surface. This also indicates a need for detailed simulation.

4. SUMMARY

The presence of a large range of geometric length scales, chemical and physical properties and process conditions in combustion in porous media lead to a variety of thermal and chemical nonequilibria. The design of combustion processes and systems, such as, catalytic reactors and converters, direct energy and gas conversion devices and systems, chemical sensors and materials synthesis processes requires the ability to model the processes, capturing the important phenomena. When there is sufficient separation of the geometric and phenomenologic length scales, the use of volume-averaged models empirically extended to treat large variations of temperature and chemical potential at the pore or particle-level sufices from an engineering point of view. However, when there is no separation among the various length scales, there is a need for local, detailed simulation.

In particular, the increase in the conversion rate of trace pollutants for catalytic converters, depends on the optimization of the porous structure and catalytic-site distribution for large surface area and low resistance to mass diffusion. Bimodal pore-size distributions with axial and transversal nonuniform crystallite distribution may lead to an optimum performance. Depending on the regime of operation, detailed simulation may be needed to complement the average models. Likewise, the ability to model and implement new design ideas, like the optimal fuel distribution in porous burners, optimization of geometric characteristics of the solid matrix in thermal regeneration devices, the suppression or augmentation of the pyrolysis in solid combustion and the control of the nonuniform distribution of reactants in combustion synthesis will lead to the development of more efficient combustion systems and processes.

References

[1] T. Takeno and K. Sato, <u>Combust. Sci. Technol.</u>, v.20, pp.73-84 (1979).

[2] Y. Yoshizawa, S. Kiyoshi and R. Echigo, <u>Int. J. Heat Mass Transfer</u>, v.31, pp.311-319 (1988).

[3] S. B. Sathe, R. E. Peck and T. W. Tong, <u>Int. J. Heat Mass Transfer</u>, v.33, pp.1331-1338 (1990).

[4] R. Echigo, R., "Radiation enhanced/controlled phenomena of heat and mass transfer in porous media," *Proceedings of the 1st ASME/JSME Joint Thermal Engineering Conference*, v.4, pp.xxi-xxxii (1991).

[5] P. Hsu and R. D. Matthews, <u>Combustion and Flame</u>, v.93, pp.457-466 (1993).

[6] M. Sahraoui and M. Kaviany, <u>Int. J. Heat and Mass Transfer</u>, v.37, pp.2817-2834 (1994).

[7] T. W. Tong and W. Li, <u>J. Quant. Spectrosc. Radiat. Transfer</u>, v.53, pp.235-248 (1995).

[8] J. R. Howell, M. J. Hall and J. L. Ellzey, <u>Prog. Energy Combust. Sci.</u>, v.22, pp.121-145 (1996).

[9] E. Koberstein and G. Wannemacher, *Catalysis and Automotive Pollution Control*, SAE, pp.155-172 (1987)

[10] J. N. Armor, <u>Catalysis Today</u>, v.26, pp.99-105 (1995).

[11] W. C. Pfefferle adn L. D. Pfefferle, <u>Prog. Energy Combust. Sci.</u>, v.12, pp.25-41 (1986).

[12] P. Markatou, L. D. Pfefferle and M. D. Smooke, <u>Combustion and Flame</u>, v.93, pp.185-201 (1993).

[13] L. D. Pfefferle, <u>Catalysis Today</u>, v.26, pp.255-265 (1995).

[14] K. Eguchi and H. Arai, <u>Catalysis Today</u>, v.29, pp.379-386 (1996).

[15] D. A. Hickman and L. D. Schmidt, <u>AIChE Journal</u>, v.39, pp.1164-1177 (1993).

[16] M. Ziauddin, A. Balakrishna, D. G. Vlachos and L. D. Schmidt, <u>Combustion and Flame</u>, v.110, pp.377-391 (1997).

[17] A. Ferrenberg, <u>AIAA Journal</u>, AIAA 90-2510 (1990).

[18] A. Ferrenberg, <u>SAE Transactions</u>, SAE 940946 (1994).

[19] K. Hanamura, K. Bohda and Y. Miyairi, <u>Energy Convers. Mgmt.</u>, v.38, pp.1259-1266 (1997).

[20] G. A. Fateev and O. S. Rabinovich, <u>Int. J. Hydrogen Energy</u>, v.27, pp.915-924 (1997).

[21] C.-W. Park and M. Kaviany, *Proceedings of the 1999 National Heat Transfer Conference*, Albuquerque, New Mexico (1999).

[22] K. Hanamura, K. Akagi and K. Koyanagi, *Proceedings of the 5th ASME/JSME Joint Thermal Engineering Conference*, pp.1-6, San Diego, California (1999).

[23] C.-W. Park and M. Kaviany, *Optimization of High-Temperature Radiant Burner*, Report to Air Liquide, CRCD, Joay-en-Josas, France (1999).

[24] R. J. Farrauto, <u>React. Kinet. Catal. Lett.</u>, v.60, pp.233-241 (1997).

[25] A. C. MacIntosh, M. Bains, W. Crocombe and J. F. Griffiths, <u>Combustion and Flame</u>, v.99, pp.541-550 (1994).

[26] M. Kaplan and M. J. Hall, <u>Experimental Thermal and Fluid Science</u>, v.11, pp.13-20 (1995).

[27] V. V. Martynenko, R. Echigo and M. Yoshida, <u>Int. J. Heat Mass Transfer</u>, v.41, pp.117-126 (1998).

[28] C. Di Blasi, <u>Combust. Sci. and Tech.</u>, v.90, pp.315-340 (1993).

[29] D. A. Schult, B. J. Matkowski, V. A. Volpert and A. C. Fernandez-Pello, <u>Combustion and Flame</u>, v.104, pp.1-26 (1996).

[30] C. Brereton, <u>Resources, Conservation and Recycling</u>, v.16, pp.227-264 (1996).

[31] M. Fatehi and M. Kaviany, <u>Int. J. Heat and Mass Transfer</u>, v.40, pp.2607-2620 (1997).

[32] C. P. Garner and J. C. Dent, <u>SAE Transactions</u>, SAE Paper No. 880007 (1988).

[33] R. Noirot, P. Gilot, R. Gadiou, and G. Prado, <u>Combust. Sci. Tech.</u>, v.95, pp.139-160 (1994).

[34] Z. A. Munir, <u>Ceramic Bulletin</u>, v.67, pp.342-349 (1988).

[35] A. Varma and J.-P. Lebrat, <u>Chem. Eng. Sci.</u>, v.47, pp.2179-2193 (1992).

[36] K. Brezinski, *Proceedings of the Twenty-Sixth Symposium (International) on Combustion/The Combustion Institute*, pp.1805-1816 (1996).

[37] M. Wooldridge, <u>Prog. Energy Combust. Sci.</u>, v.24, pp.63-87 (1998).

[38] A. A. M. Oliveira and M. Kaviany, <u>Int. J. Heat Mass Transfer</u>, v.42, pp.1059-1073 (1999).

[39] A. A. M. Oliveira and M. Kaviany, <u>Int. J. Heat Mass Transfer</u>, v.42, pp.1075-1095 (1999).

[40] R. Armstrong, <u>Combust. Sci. Tech.</u>, v.71, pp.155-174 (1990).

[41] S. Whitaker, *Advances in Heat Transfer*, v.7, pp.119-203, edited by J. P. Hartnett and I. Irvine, Academic Press, New York (1977).

[42] M. Quintard and S. Whitaker, <u>Transport in Porous Media</u>, v.3, pp.357-413 (1988).

[43] M. Quintard and S. Whitaker, *Advances in Heat Transfer*, v.23, pp.369-464, edited by J. P. Hartnett and T. F. Irvine, Academic Press (1993).

[44] M. Quintard and S. Whitaker, <u>Chem. Engng. Sci.</u>, v.48, pp.2537-2564 (1993)

[45] M. Quintard and S. Whitaker, <u>Transport in Porous Media</u>, v.14, pp.179-206 (1994).

[46] M. Quintard, M. Kaviany and S. Whitaker, <u>Advances in Water Resources</u>, v.20, pp.77-94 (1997).

[47] M. Kaviany, *Principles of Heat Transfer in Porous Media*, Springer-Verlag, Corrected 2nd Ed., (1999).

[48] S. Zhdanov, L. A. Kennedy and G. Koester, <u>Combustion and Flame</u>, v.100, pp.221-231 (1995).

[49] A. P. Aldushin, I. E. Rumanov and B. J. Matkowsky, <u>Combustion and Flame</u>, v.118, pp.76-90 (1999).

[50] F. J. Keil and C. Rieckmann, <u>Chemical Engineering Science</u>, v.49, pp.4811-4822 (1994).

[51] M. Sahimi, <u>Physics Reports</u>, v.306, pp.213-395 (1998).

[52] L. Zhang and N. A. Seaton, <u>Chemical Engineering Journal</u>, v.49, pp.41-50 (1994).

[53] V. Alvarado, H. T. Davis and L. E. Scriven, <u>Chemical Engineering Science</u>, v.52, pp.2865-2881 (1997).

[54] M.-O. Coppens and G. F. Froment, <u>Chem. Eng. Sci.</u>, v.50, pp.1027-1039 (1995).

[55] R. B. Bird, W. E. Stewart, and E. N. Lightfoot, *Transport phenomena*, John Wiley, New York (1960).